

# Entangled states from simple quantum graphs

Alison A. Silva<sup>1,\*</sup>, D. Bazeia<sup>2,†</sup> and Fabiano M. Andrade<sup>1,3,‡</sup>

<sup>1</sup>*Programa de Pós-Graduação em Ciências/Física, Universidade Estadual de Ponta Grossa, 84030-900 Ponta Grossa, Paraná, Brazil*

<sup>2</sup>*Departamento de Física, Universidade Federal da Paraíba, 58051-900 João Pessoa, Paraíba, Brazil*

<sup>3</sup>*Departamento de Matemática e Estatística, Universidade Estadual de Ponta Grossa, 84030-900 Ponta Grossa, Paraná, Brazil*  
(Dated: March 7, 2025)

This work deals with quantum transport in open quantum graphs with two scattering channels. They are used as a two-level system whose weights are defined by its reflection and transmission amplitudes. We propose a controlled operation between two quantum graphs, where the scattering in a quantum graph modifies the second one, changing its outcome. Our findings show that the scattering measurements in this system are linked to recent results on randomized quantum graphs. The main results reveal the presence of entangled states according to the wave-number values in each quantum graph and the applied controlled operation. It was possible to determine the criteria for maximal entanglement or separability. In particular, we uncovered the presence of entanglement in a simple system consisting of two simple quantum graphs, with only one edge and a controlled phase.

## I. INTRODUCTION

Quantum graphs [1, 2] have been used to describe different phenomena in several areas of science. In particular, they may arise as simplified models in chemistry, mathematics, and physics and have become a powerful tool for studying different aspects of the natural world. Specific subjects include the study of quantum chaos [3, 4], Anderson localization [5], and chaotic and diffusive scattering [6, 7], to name just a few possibilities of current interest.

In this work, we focus mainly on a novel investigation concerning the construction of a direct connection between quantum graphs (QGs) and quantum systems within the quantum information framework. To be more specific, we shall deal with scattering processes in QGs equipped with two scattering channels and their relation with two-level quantum systems. This is perhaps the simplest possibility, and extensions involving three or more states will be considered elsewhere. The purpose of this study is to relate properties of the quantum states generated by a given QG and their possible connections to the two-level quantum states they generate. The construction can allow us to define some controlled operations between the QGs, which will be used to infer properties of the two-level quantum system on the quantum information side. Other approaches, which use the scattering matrix for quantum computation have been described before in [8, 9], but the procedure and the results we describe in the present work are original.

To implement the present investigation, we first deal with the methodology in Sec. II, where some basic information on quantum graphs can be found, together with an explanation on how the scattering amplitudes are calculated for a QG, enabling us to obtain the corresponding scattering matrix. We go on and in Sec. III we discuss how the scattering results can be utilized to define a quantum state. Next, we introduce an

interaction between the two quantum graphs by a controlled operation between these graphs and use the entanglement entropy in order to verify the limits where the state is separable or maximally entangled, in terms of the scattering amplitudes. In Sec. IV, we further explore the results investigating several examples of quantum graphs and obtaining other results related to the corresponding graph structures. We then close the work in Sec. V, summarizing the main results and including possible directions for future investigations.

## II. METHODOLOGY

A graph  $G = (V, E)$  is defined as a pair consisting of a finite set of vertices  $V = \{v_1, \dots, v_n\}$  and a set of edges  $E = \{e_1, \dots, e_l\}$  [10]. The order of a graph is the number of vertices denoted by  $|V| = n$  and the size of the graph is the number of edges denoted by  $|E| = l$ . Moreover, the topology of the graph is defined by its adjacency matrix, which is defined as

$$A(G) = \begin{cases} 1, & \text{if } i \sim j \\ 0, & \text{otherwise} \end{cases} \quad (1)$$

with  $i \sim j$  indicating that  $i$  is adjacent to  $j$ .

A quantum graph is a triple  $\{\Gamma_G, H, BC\}$  consisting of a metric graph  $\Gamma_G$ , obtained from a graph  $G$  where we assign positive lengths  $\ell_{e_j} \in (0, \infty)$  to each edge of the graph, a differential operator,  $H$ , and a set of boundary conditions (BCs) at the vertices, which defines the individual scattering amplitudes at the vertices [2]. We consider the stationary free Schrödinger operator  $H = -(\hbar^2/2m)d^2/dx^2$  on each edge, and we use standard BCs (Neumann-Kirchhoff) on the corresponding vertices [2, 11]. Then, to create an open quantum graph with two scattering channels,  $\Gamma_G^2$ , we add two leads (semi-infinite edges) to two different vertices. The open quantum graph  $\Gamma_G^2$  then represents a scattering system with two scattering channels, which is characterized by the global energy-dependent scattering matrix  $\sigma_{\Gamma_G^2}^{(f,i)}(k)$ , where, as usual,  $k = \sqrt{2mE/\hbar^2}$  is the wave number, with  $i$  and  $f$  being the entrance and exit scattering channels, respectively.

\* alisonantunessilva@gmail.com

† bazeia@fisica.ufpb.br

‡ fmandrade@uepg.br

In general, for an open quantum graph with  $c$  scattering channels, we can obtain the global scattering amplitudes  $\sigma_{\Gamma_G}^{(f,i)}(k)$  by employing the Green's function approach developed in Refs. [12, 13]. This approach is general and has been successfully used in several transport studies in quantum graphs [14–19], and to model the transport in filament switching [20]. The exact scattering Green's function for a quantum signal of fixed wave number  $k$ , with initial position  $x_i$  in the lead  $l_i$  and final position  $x_f$  in the lead  $l_f$  can be obtained by using the adjacency matrix of the underlying graph [13]. Thus, the exact Green's function is written as

$$G_{\Gamma_G^2}(x_f, x_i; k) = \frac{m}{i\hbar^2 k} \sigma_{\Gamma_G}^{(f,i)}(k) e^{ik(x_i + x_f)}, \quad (2)$$

where

$$\sigma_{\Gamma_G}^{(f,i)}(k) = r_i(k) \delta_{i,f} + \sum_{j \in E_i} A_{ij} p_{ij}(k) t_j(k), \quad (3)$$

is the global scattering amplitude from a lead  $l_i$  to a lead  $l_f$ , with  $p_{ij}(k)$  the family of paths between the vertices  $i$  and  $j$ , which are given by

$$p_{ij}(k) = z_{ij} p_{ji} r_j(k) + \sum_{l \in E_j^m} z_{ij} A_{jl} p_{jl} t_l(k) + z_{ij} \delta_{jn} t_n(k), \quad (4)$$

with  $z_{ij} = e^{ik\ell_{(i,j)}}$  and  $\ell_{(i,j)}$  the length of the edge between vertices  $i$  and  $j$ . The family  $p_{ji}(k)$  is given by the same expression above, but with the swapping of indices  $i$  and  $j$ . Then, in each vertex  $i$  we associate one  $p_{ij}(k)$  for every  $j \in E_i$ , where  $E_i$  is the set of adjacent vertices of  $i$ . In the above equation,  $r_i(k)$  and  $t_i(k)$  are the individual reflection and transmission amplitudes, respectively, associated with the boundary conditions imposed at the vertex  $i$ . For the standard BC, the individual quantum amplitudes are independent of  $k$ , and are explicitly given by  $r_i = (2/d_i) - 1$  and  $t_i = 2/d_i$ , with  $d_i$  the degree of the vertex  $i$ .

For a quantum graph  $\Gamma_G^2$  with two scattering channels (represented by  $\Gamma_G$  to simplify the notation), which will be labeled as  $l_0$  and  $l_1$ , the scattering  $S$ -matrix is defined in terms of the global scattering amplitudes, i.e.,

$$S_{\Gamma_G} = \begin{pmatrix} \sigma_{\Gamma_G}^{(0,0)} & \sigma_{\Gamma_G}^{(0,1)} \\ \sigma_{\Gamma_G}^{(1,0)} & \sigma_{\Gamma_G}^{(1,1)} \end{pmatrix}. \quad (5)$$

For the purpose of the present study and using the time reversal symmetry of the scattering, we can simplify the notation for the scattering quantum amplitudes using  $\sigma_{\Gamma_G}^{(0,0)} = \sigma_{\Gamma_G}^{(1,1)} = r_G$ ,  $\sigma_{\Gamma_G}^{(0,1)} = \sigma_{\Gamma_G}^{(1,0)} = t_G$ , where the  $r_G$  and  $t_G$  are the global scattering amplitudes of the quantum graph  $\Gamma_G$  associated with the graph  $G$ .

### III. QUANTUM SCATTERING STATES

We now label the two scattering channels of the system as the quantum states  $|0\rangle$  and  $|1\rangle$ . Defining an initial state as a signal entering from the lead labeled  $l_0$ , its initial state is  $|\psi_i\rangle =$



FIG. 1. The scattering in QGs as an information model. Initially there is an input state in a given QG  $\Gamma_G$ , where a particle enters by one of its leads, called as lead  $l_0$  and thus the particle is found to be in the state  $|0\rangle$ . After the scattering in  $\Gamma_G$ , there is an output state where the particle have two scattering amplitudes:  $r_G$  to reflect to the same lead  $l_0$  and thus it is in the state  $|0\rangle$ ; and  $t_G$  to transmit through the QG and be found in the other lead  $l_1$ , being in the state  $|1\rangle$ .

$|0\rangle$ . After the scattering in a QG with 2 scattering channels  $\Gamma_G$  and scattering matrix  $S_{\Gamma_G}$ , that state becomes

$$\begin{aligned} |\Gamma_G\rangle &= S_{\Gamma_G} |0\rangle, \\ &= r_G |0\rangle + t_G |1\rangle, \end{aligned} \quad (6)$$

where  $|\Gamma_G\rangle$  is the resulting state after the scattering process. This is illustrated in Fig. 1 where initially there is an input state  $|0\rangle$ , and after the scattering the output state is  $r_G |0\rangle + t_G |1\rangle$ .

In order to describe the main idea of the present work, we have to deal with two QGs. In the standard language of quantum information, it is common to describe a pair of systems  $A$  and  $B$  by Alice and Bob [21]. In this sense, let us introduce two QGs, Alice's QG ( $\Gamma_A$ ) and Bob's QG ( $\Gamma_B$ ). The states in each of these systems are defined by  $|\Gamma_i\rangle = S_i |0_i\rangle$ . Now, let us define Alice's QG as the controller, while Bob's QG is the one being controlled. When the state measured in  $\Gamma_A$  is  $|0\rangle_A$ , there will be no changes in Bob's QG, which is defined as  $|\Gamma_B\rangle$ . But when  $|1\rangle_A$  is measured in Alice's system, some modification is applied in Bob's QG, modifying it from  $\Gamma_B$  to  $\Gamma_{B'}$ . These modifications can include edge length changes, potential applied on its edges, changes in the boundary conditions of the vertices, and so forth.

The operator that makes these controlled changes in the QG system can be represented by  $CS_{B,B'}^A$ , which is given by

$$CS_{B,B'}^A = |0_A\rangle\langle 0_A| \otimes S_{\Gamma_B} + |1_A\rangle\langle 1_A| \otimes S_{\Gamma_{B'}}, \quad (7)$$

i.e., a controlled gate that performs the modification  $\Gamma_B \rightarrow \Gamma_{B'}$

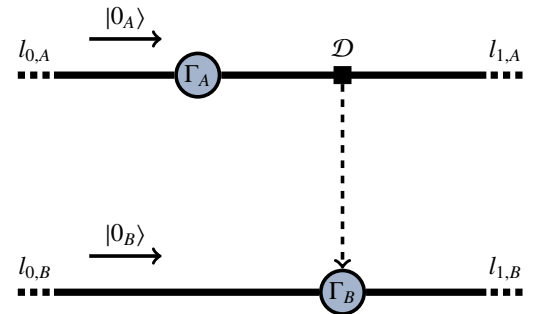


FIG. 2. The interaction model between the two QGs  $\Gamma_A$  and  $\Gamma_B$  by a controlled gate, where a coherent interaction denoted  $\mathcal{D}$  may change  $\Gamma_B$  to  $\Gamma_{B'}$ .

according to the measured state of  $|\Gamma_A\rangle$ . Thus, the QG interaction state, which is illustrated in Fig. 2, can be written as

$$|\Psi_{AB}\rangle = CS_{B,B'}^A |0_A\rangle \otimes |0_B\rangle, \quad (8)$$

$$= r_A |0_A\rangle \otimes |\Gamma_B\rangle + t_A |1_A\rangle \otimes |\Gamma_{B'}\rangle. \quad (9)$$

When  $|\Gamma_{B'}\rangle = |\Gamma_B\rangle$ , the state is easily separable as  $|\Psi_{AB}\rangle = |\Gamma_A\rangle \otimes |\Gamma_B\rangle$ .

However, since we want to define a more general situation, where another possibility may occur, using the shorthand notation  $|i_A\rangle \otimes |j_B\rangle = |i, j\rangle$ , we can write the scattering state as

$$|\Psi_{AB}\rangle = r_A r_B |0, 0\rangle + r_A t_B |0, 1\rangle + t_A r_{B'} |1, 0\rangle + t_A t_{B'} |1, 1\rangle. \quad (10)$$

In this case, the density matrix  $\rho = |\Psi\rangle\langle\Psi|$  has now the form

$$\rho_{AB} = \begin{pmatrix} |r_A|^2 |r_B|^2 & |r_A|^2 r_B t_B^* & r_A r_B t_A^* r_{B'}^* & r_A r_B t_A^* t_{B'}^* \\ |r_A|^2 t_B r_B^* & |r_A|^2 |t_B|^2 & r_A t_B t_A^* r_{B'}^* & r_A t_B t_A^* t_{B'}^* \\ t_A r_{B'} r_A^* r_B^* & t_A r_{B'} r_A^* t_B^* & |t_A|^2 |r_{B'}|^2 & |t_A|^2 r_{B'} t_{B'}^* \\ t_A t_{B'} r_A^* r_B^* & t_A t_{B'} r_A^* t_B^* & |t_A|^2 t_{B'} r_{B'}^* & |t_A|^2 |t_{B'}|^2 \end{pmatrix}. \quad (11)$$

Alice's measurements can be verified by taking the partial trace over Bob's subsystem, and simplifying with  $|r_j|^2 + |t_j|^2 = 1$ . The result becomes

$$\rho_A = \begin{pmatrix} |r_A|^2 & r_A t_A^* (r_B r_{B'}^* + t_B t_{B'}^*) \\ t_A r_A^* (r_B r_{B'}^* + t_B t_{B'}^*) & |t_A|^2 \end{pmatrix}. \quad (12)$$

As Alice have the controller system, the measurements in each channel will return  $|r_A|^2$  and  $|t_A|^2$ .

On the other hand, if one takes the partial trace over the Alice's subsystem, we obtain the reduced density matrix related to Bob's measurements

$$\rho_B = \begin{pmatrix} |r_A|^2 |r_B|^2 + |t_A|^2 |r_{B'}|^2 & |r_A|^2 r_B t_B^* + |t_A|^2 r_{B'} t_{B'}^* \\ |r_A|^2 t_B r_B^* + |t_A|^2 t_{B'} r_{B'}^* & |r_A|^2 |t_B|^2 + |t_A|^2 |t_{B'}|^2 \end{pmatrix}. \quad (13)$$

We use this result to obtain the expected transmission value in Bob's QG in the form

$$\langle 1 | \rho_B | 1 \rangle = |r_A|^2 |t_B|^2 + |t_A|^2 |t_{B'}|^2. \quad (14)$$

If we introduce the parameter  $p$  and define it as  $p = |t_A|^2$ , it is possible to rewrite the above expression as

$$\langle 1 | \rho_B | 1 \rangle = (1 - p) |t_B|^2 + p |t_{B'}|^2. \quad (15)$$

This result shows that the measurements in Bob's QG scattering channels can be studied as a linear combination of the scattering probabilities of the system in the two possible situations. Interestingly, an approach to studying scattering in quantum graphs in the presence of a randomization parameter  $p$  was very recently presented in [19]. There, the parameter  $p$  was used as a randomization parameter defining probability of the existence of edges in a given QG, leading to the same transmission. Here, however, we note that  $p$  may be used to describe the interaction between Alice and Bob QGs, indicating that the result may have expanded practical importance.

## A. Entanglement entropy

The definition for the von Neumann entropy related to the density matrix  $\rho$  is given by

$$H(\rho) = -\text{Tr}(\rho \log_2 \rho). \quad (16)$$

When applied to the reduced density matrix  $\rho_A$  of a system formed by two subsystems  $A$  and  $B$ , one can follow Refs. [21–23] in order to introduce the entanglement entropy in the form

$$H(\rho_A) = -\sum_j \lambda_j \log_2 \lambda_j, \quad (17)$$

where  $\lambda_j$  is used to identify the eigenvalues of  $\rho_A$ . Thus, taking this entropy with  $A$  being a two-level system, with eigenvalues  $\{\lambda_+, \lambda_-\}$ , we have

$$H(\rho^A) = -\lambda_+ \log_2 \lambda_+ - \lambda_- \log_2 \lambda_-. \quad (18)$$

This can be applied to the reduced density matrix from Eq. (12) which has eigenvalues

$$\lambda_{\pm} = \frac{1}{2} \left( 1 \pm \sqrt{(|r_A|^2 - |t_A|^2)^2 + 4 |r_A|^2 |t_A|^2 |r_B r_{B'}^* + t_B t_{B'}^*|^2} \right). \quad (19)$$

As one knows, this entanglement entropy will be maximized when the eigenvalues are equal. This imposes that

$$\sqrt{(|r_A|^2 - |t_A|^2)^2 + 4 |r_A|^2 |t_A|^2 |r_B r_{B'}^* + t_B t_{B'}^*|^2} = 0. \quad (20)$$

After some manipulation, using  $|r_A|^2 = 1 - |t_A|^2$  we can write

$$|r_A|^2 |t_A|^2 \left( 1 - |r_B r_{B'}^* + t_B t_{B'}^*|^2 \right) = \frac{1}{4}. \quad (21)$$

The only solution is obtained for  $|r_A|^2 = |t_A|^2 = 1/2$ , and

$$|r_B r_{B'}^* + t_B t_{B'}^*|^2 = 0. \quad (22)$$

It shows that Alice's QG must have maximal scattering entropy [16–18], while the restriction in Bob's QG given by Eq. (22) indicates that to achieve maximal entanglement entropy, the change in the scattering amplitudes on  $\Gamma_B$  should be such that  $|t_{B'}|^2 = |r_B|^2$  and, consequently,  $|r_{B'}|^2 = |t_B|^2$ , that is, a swap between its scattering probabilities. Moreover, when

$$|r_A|^2 |t_A|^2 \left( 1 - |r_B r_{B'}^* + t_B t_{B'}^*|^2 \right) = 0, \quad (23)$$

the entanglement entropy is zero and the system is separable. This is obtained if the transmission or the reflection probability is zero in Alice's QG, or when  $|r_B r_{B'}^* + t_B t_{B'}^*|^2 = 1$ , which can be obtained when there is no change in the Bob's QG scattering amplitudes or when a global phase is applied or even when a phase  $2\pi n$  is added to one of these scattering amplitudes. Summing up, the entanglement entropy of the system vanishes when the scattering entropy in the Alice's QG is zero, or if the operation included in the Bob's QG is equivalent to a global phase.

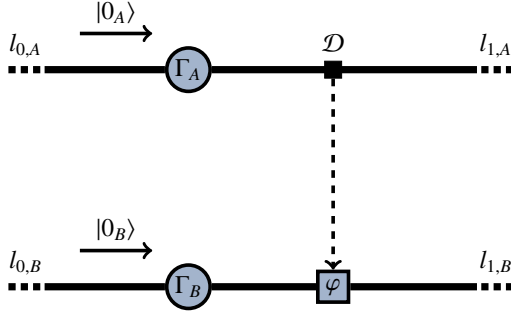


FIG. 3. The controlled scattering system of two quantum graphs  $\Gamma_A$  and  $\Gamma_B$ , where the controlled operation is a phase  $\varphi$  applied to the scattering channel  $l_{1,B}$  by a coherent detection  $\mathcal{D}$  in the scattering channel  $l_{1,A}$ .

#### IV. RESULTS

Let us now include a controlled change in Bob's QG as a phase  $\varphi$  applied to its transmission channel. This is illustrated in Fig. 3. In this way, Eq. (10) becomes

$$|\Psi_{AB}\rangle = r_A r_B |0, 0\rangle + r_A t_B |0, 1\rangle + t_A r_B |1, 0\rangle + e^{i\varphi} t_A t_B |1, 1\rangle. \quad (24)$$

For the maximal entanglement obtained from Eq. (21), we find that this new system may present maximal entanglement when

$$|r_A|^2 |t_A|^2 \left(1 - |r_B|^2 + e^{-i\varphi} |t_B|^2\right) = \frac{1}{4}. \quad (25)$$

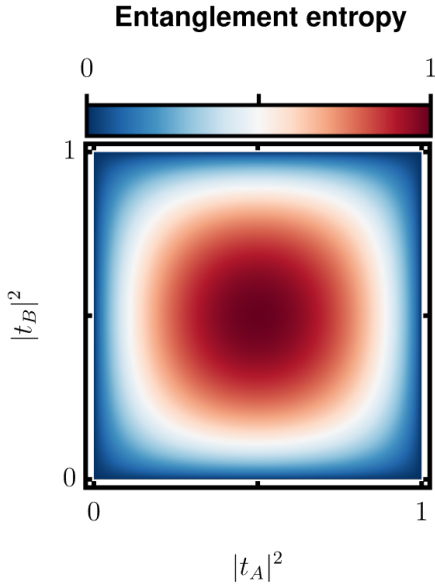


FIG. 4. The entanglement entropy as function of the transmission probability  $|t_A|^2$  and  $|t_B|^2$  in each QG when a controlled phase  $\pi$  is applied in Bob's QG, with  $t_B = -t_B$ .

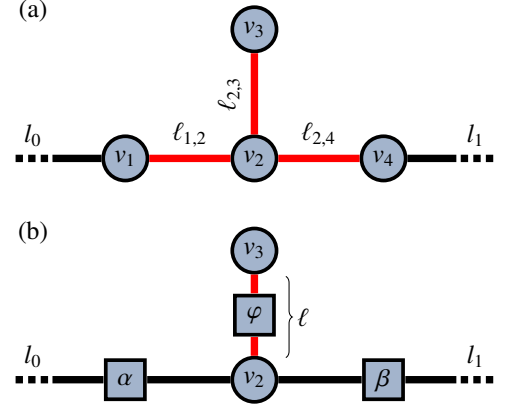


FIG. 5. (a) A star quantum graph with four vertices ( $S_4$ ) and two scattering channels ( $\Gamma_{S_4}$ ) which are connected to the vertices labeled as 1 and 4. Each edge  $e_{i,j}$ , which connects a pair of vertices  $\{i, j\}$  in the QG has a given length  $\ell_{i,j}$ . (b) An equivalent QG where a phase shift operation  $\alpha$  is used to mimic the phase obtained due the length  $\ell_{1,2}$ , and the same is done to  $\ell_{2,4}$ , being replaced by  $\beta$ . The distance between the vertices  $v_2$  and  $v_3$  is  $\ell$  and a possible phase shift operation along this edge is defined by  $\varphi$ .

Interestingly, we can find a solution with a real  $\varphi$  with  $|r_A|^2 = |t_A|^2 = 1/2$ ,  $|r_B|^2 = |t_B|^2 = 1/2$  and  $\varphi = (2n+1)\pi$ . This is equivalent to applying a controlled-Z gate together with some unitary operation in each system because of all the possible scattering amplitudes that satisfy these conditions. Furthermore, from the separability condition obtained in Eq. (23), one notices this new system will be separable for

$$|r_A|^2 |t_A|^2 \left(1 - |r_B|^2 + e^{-i\varphi} |t_B|^2\right) = 0. \quad (26)$$

This is obtained when  $|r_A|^2 = 0$ , or  $|t_A|^2 = 0$  or  $\varphi = 2n\pi$ . The entanglement entropy for this system is illustrated in Fig. 4, where we have considered  $\varphi = \pi$ .

We can also consider the case where a controlled phase acts inside the quantum graph. In order to do that, let us now study the simple case of star quantum graphs. First, we consider the scattering amplitudes in the quantum graph presented in Fig. 5 (a). The corresponding scattering matrix is given by

$$S_{\Gamma_{S_4}} = \frac{-1}{2i + \tan(k\ell_{2,3})} \begin{pmatrix} \tan(k\ell_{2,3}) e^{2ik\ell_{1,2}} & -2ie^{ik(\ell_{1,2}+\ell_{2,4})} \\ -2ie^{ik(\ell_{1,2}+\ell_{2,4})} & \tan(k\ell_{2,3}) e^{2ik\ell_{2,4}} \end{pmatrix}. \quad (27)$$

As the lengths  $\ell_{1,2}$  and  $\ell_{2,4}$  contributes only to phase increment on the scattering amplitudes, it is interesting to simplify them to some phase equivalent parameters  $\alpha = k\ell_{1,2}$  and  $\beta = k\ell_{2,4}$ . In the same way, we can rewrite the length  $\ell_{2,3}$  as simply  $\ell$  and add a possible phase inclusion  $\varphi$ , obtaining  $k\ell_{2,3} = k\ell + \varphi$ . An illustration for these changes is shown in Fig. 5(b). Thus, using this modifications the scattering matrix is given by

$$S_{\Gamma_{S_4}} = \frac{-1}{2i + \tan(k\ell + \varphi)} \begin{pmatrix} \tan(k\ell + \varphi) e^{2i\alpha} & -2ie^{i(\alpha+\beta)} \\ -2ie^{i(\alpha+\beta)} & \tan(k\ell + \varphi) e^{2i\beta} \end{pmatrix}. \quad (28)$$

If one takes  $k\ell + \varphi = n_{k\ell}\pi \pm \arctan(2)$ , for  $n_{k\ell}$  integer, together with some phase shift on each scattering state, which can be

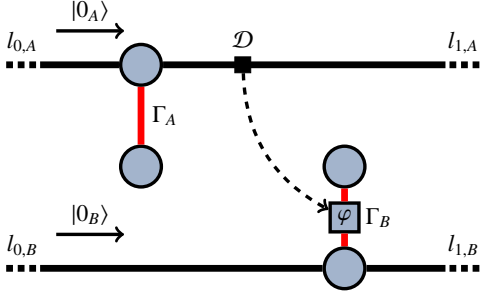


FIG. 6. Illustration of the system composed by two QGs  $\Gamma_A$  and  $\Gamma_B$ , where a controlled phase shift  $\varphi$ , activated by a coherent detection  $\mathcal{D}$ , is applied to the shown edge of  $\Gamma_B$ .

manipulated by the  $\alpha$  and  $\beta$  variables, this matrix may become the Hadamard matrix. Indeed, this is achieved, for instance, after taking  $k\ell + \varphi = \arctan(2)$ ,  $\alpha = 5\pi/8$  and  $\beta = 9\pi/8$ .

We now consider the simpler possibility, taking  $\varphi = 0$  and using the values  $\alpha = n_\alpha\pi$  and  $\beta = n_\beta\pi$ , with integers  $n_\alpha$  and  $n_\beta$ . This leads to the scattering matrix in the form

$$S_{\Gamma_{S_4}} = \frac{-1}{2i + \tan(k\ell)} \begin{pmatrix} \tan(k\ell) & -2i \\ -2i & \tan(k\ell) \end{pmatrix}. \quad (29)$$

From that we can extract the quantum amplitudes

$$\mathcal{R}(k\ell) = -\frac{\tan(k\ell)}{2i + \tan(k\ell)}, \quad (30)$$

and

$$\mathcal{T}(k\ell) = \frac{2i}{2i + \tan(k\ell)}. \quad (31)$$

For the interaction between two of these QGs, we suppose that Alice's and Bob's QG are initially two identical QGs as defined before as a star quantum graph with four vertices, illustrated in Fig. 5, each one with a wave number  $k_A$  and  $k_B$ . Moreover, we introduce a controlled operation in Bob's QG as an extra phase  $\phi$  operation along the edge  $e_{2,3}$ . This is illustrated in Fig. 6. Thus, the scattering state in this system is given by

$$|\Psi_{AB}\rangle = \mathcal{R}(k_A\ell)\mathcal{R}(k_B\ell)|0, 0\rangle + \mathcal{R}(k_A\ell)\mathcal{T}(k_B\ell)|0, 1\rangle + \mathcal{T}(k_A\ell)\mathcal{R}(k_B\ell + \phi)|1, 0\rangle + \mathcal{T}(k_A\ell)\mathcal{T}(k_B\ell + \phi)|1, 1\rangle. \quad (32)$$

Its entanglement entropy is illustrated in Fig. 7 as function of  $k_A\ell$ ,  $k_B\ell$  and  $\phi$ . From the condition for maximal entanglement entropy, as we found in Eq. (21), we have that  $|r_A|^2 = |t_A|^2 = 1/2$ , which is obtained for  $k_A\ell = n_{k_A}\pi \pm \arctan(2)$ , together with the equality  $|r_B r_B^* + t_B t_B^*|^2 = 0$ , which is fulfilled with

$$\tan(k_B\ell) \tan(k_B\ell + \phi) = -4. \quad (33)$$

This leads to the solution

$$\phi = -\arctan\left(\frac{3 \sin(2k_B\ell)}{5 + 3 \cos(2k_B\ell)}\right) + (2n + 1) \frac{\pi}{2}. \quad (34)$$

When one of the conditions  $|t_A|^2 = 0$ , or  $|r_A|^2 = 0$ , or  $|r_B|^2 = 0$ , or  $|t_B|^2 = 0$  or  $\phi = 2n\pi$  is satisfied, the state is separate.

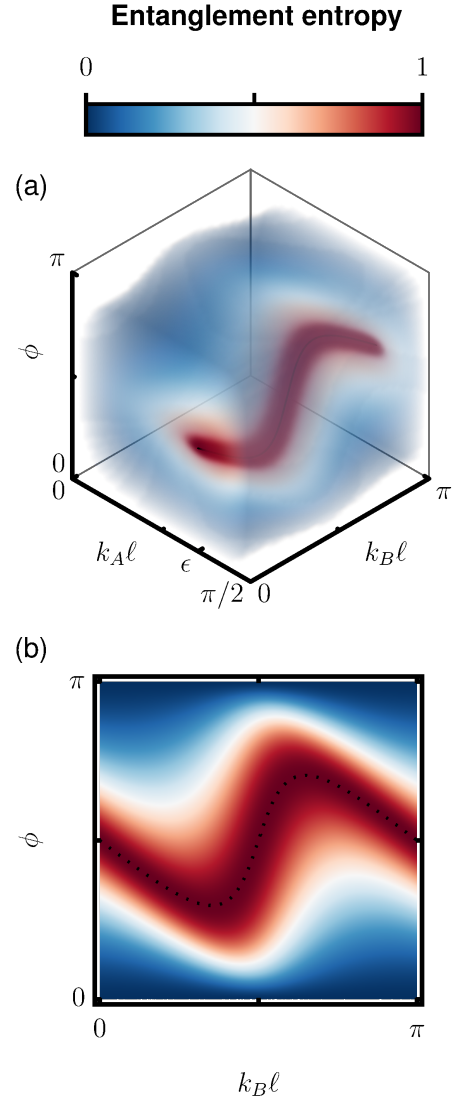


FIG. 7. The entanglement entropy in a system with two QGs, with wavenumber  $k_A$  and  $k_B$ , when a controlled phase  $\phi$  is applied in the edge of Bob's QG, as illustrated in Fig. 6. (a) The case with the three variables  $k_A\ell$ ,  $k_B\ell$  and  $\phi$ . (b) The case with  $k_A\ell = \epsilon = \arctan(2)$ , highlighting the maximal entropy by a black dotted line.

## V. ENDING COMMENTS

We have developed a procedure for the entanglement of two QGs considering a coherent interaction between them. We exemplified two cases using controlled operations of phase shift in the transmission channel and inside of the QGs edges. We have shown that the scattering conditions to obtain entanglement in those systems. We think that the results of the present work are original and of practical interest. Other possible modifications to QGs, such as edge length, boundary conditions on its vertices, or potential along its edges, may serve to generate entangled states with controllable parameters.

Other investigation possibilities may be related to the connection with scattering in randomized QGs studied in Ref.

[19]. It is also interesting to deal with controlled operations on multiple edges on the same QG or even consider three or more QGs, and graphs with three or more leads, to describe entanglement in the more general case of qudits. Moreover, QGs have applications in microwave networks [24–26]. Thus, microwave networks can be employed to measure the quantum entanglement between QGs as introduced in this work. To implement the coherent interaction that we considered in the present work, in microwave networks, one may treat the devices with a phase shifter [27, 28] or a microwave cavity [29] to simulate the required interaction. In this sense, it seems that microwave networks may be a novel source to investigate

entanglement.

## ACKNOWLEDGMENTS

This work was partially supported by Coordenação de Aperfeiçoamento de Pessoal de Nível Superior (CAPES, Finance Code 001). It was also supported by Conselho Nacional de Desenvolvimento Científico Tecnológico (CNPq) and Instituto Nacional de Ciência e Tecnologia de Informação Quântica (INCT-IQ). DB and FMA also acknowledge financial support from CNPq Grants 303469/2019-6 (DB), 402830/2023-7 (DB) and 313124/2023-0 (FMA).

- 
- [1] G. Berkolaiko, *Quantum Graphs and Their Applications: Proceedings of an AMS-IMS-SIAM Joint Summer Research Conference on Quantum Graphs and Their Applications, June 19-23, 2005, Snowbird, Utah*, Vol. 415 (American Mathematical Soc., 2006).
- [2] G. Berkolaiko and P. Kuchment, *Introduction to Quantum Graphs*, Mathematical Surveys and Monographs, Vol. 186 (American Mathematical Society, Providence, RI, 2013).
- [3] T. Kottos and U. Smilansky, Quantum chaos on graphs, *Phys. Rev. Lett.* **79**, 4794 (1997).
- [4] T. Kottos and U. Smilansky, Periodic orbit theory and spectral statistics for quantum graphs, *Ann. Phys. (NY)* **274**, 76 (1999).
- [5] H. Schanz and U. Smilansky, Periodic-orbit theory of anderson localization on graphs, *Phys. Rev. Lett.* **84**, 1427 (2000).
- [6] T. Kottos and U. Smilansky, Chaotic scattering on graphs, *Phys. Rev. Lett.* **85**, 968 (2000).
- [7] F. Barra and P. Gaspard, Transport and dynamics on open quantum graphs, *Phys. Rev. E* **65**, 016205 (2001).
- [8] R. Tevzadze and G. Giorgadze, Quantum computation with scattering matrices, *J. Math. Sci.* **153**, 197 (2008).
- [9] D. Melnikov, Knots and signal transmission in topological quantum devices, *J. Phys. Math. Theor.* **54**, 445202 (2021).
- [10] R. Diestel, *Graph Theory*, 4th ed., Graduate Texts in Mathematics Vol. 173 (Springer, 2010).
- [11] G. Berkolaiko, An elementary introduction to quantum graphs, in *Geometric and Computational Spectral Theory* (American Mathematical Society, 2017) pp. 41–72.
- [12] F. M. Andrade, A. G. M. Schmidt, E. Vicentini, B. K. Cheng, and M. G. E. da Luz, Green’s function approach for quantum graphs: an overview, *Phys. Rep.* **647**, 1 (2016).
- [13] F. M. Andrade and S. Severini, Unitary equivalence between the Green’s function and Schrödinger approaches for quantum graphs, *Phys. Rev. A* **98**, 062107 (2018).
- [14] A. Drinko, F. M. Andrade, and D. Bazeia, Narrow peaks of full transmission in simple quantum graphs, *Phys. Rev. A* **100**, 062117 (2019).
- [15] A. Drinko, F. M. Andrade, and D. Bazeia, Simple quantum graphs proposal for quantum devices, *Eur. Phys. J. Plus* **135**, 451 (2020).
- [16] A. A. Silva, F. M. Andrade, and D. Bazeia, Average scattering entropy of quantum graphs, *Phys. Rev. A* **103**, 062208 (2021).
- [17] A. A. Silva, F. M. Andrade, and D. Bazeia, Average scattering entropy for periodic, aperiodic and random distribution of vertices in simple quantum graphs, *Physica E* **141**, 115217 (2022).
- [18] A. A. Silva, F. M. Andrade, and D. Bazeia, Scattering entropies of quantum graphs with several channels, *Eur. Phys. J. Plus* **139**, 659 (2024).
- [19] A. A. Silva, D. Bazeia, and F. M. Andrade, Quantum transport in randomized quantum graphs, *APL Quantum* **1**, 046126 (2024).
- [20] A. A. Silva, F. M. Andrade, and F. Caravelli, Quantum graph models for transport in filamentary switching, *Phys. Rev. B* **111**, 045145 (2025).
- [21] R. Horodecki, P. Horodecki, M. Horodecki, and K. Horodecki, Quantum entanglement, *Rev. Modern Phys.* **81**, 865 (2009).
- [22] V. Vedral, M. B. Plenio, M. A. Rippin, and P. L. Knight, Quantifying entanglement, *Phys. Rev. Lett.* **78**, 2275 (1997).
- [23] V. Vedral and M. B. Plenio, Entanglement measures and purification procedures, *Phys. Rev. A* **57**, 1619 (1998).
- [24] O. Hul, S. Bauch, P. Pakoński, N. Savytskyy, K. Życzkowski, and L. Sirko, Experimental simulation of quantum graphs by microwave networks, *Phys. Rev. E* **69**, 056205 (2004).
- [25] T. Hofmann, J. Lu, U. Kuhl, and H.-J. Stöckmann, Spectral duality in graphs and microwave networks, *Phys. Rev. E* **104**, 045211 (2021).
- [26] A. Akhshani, M. Białous, and L. Sirko, Quantum graphs and microwave networks as narrow-band filters for quantum and microwave devices, *Phys. Rev. E* **108**, 034219 (2023).
- [27] M. Ławniczak, A. Akhshani, O. Farooq, M. Białous, S. Bauch, B. Dietz, and L. Sirko, Distributions of the wigner reaction matrix for microwave networks with symplectic symmetry in the presence of absorption, *Phys. Rev. E* **107**, 024203 (2023).
- [28] F. Arute, K. Arya, R. Babbush, D. Bacon, J. C. Bardin, R. Barends, R. Biswas, S. Boixo, F. G. Brandao, D. A. Buell, *et al.*, Quantum supremacy using a programmable superconducting processor, *Nature* **574**, 505 (2019).
- [29] Z. Wang, Z. Bao, Y. Li, Y. Wu, W. Cai, W. Wang, X. Han, J. Wang, Y. Song, L. Sun, *et al.*, An ultra-high gain single-photon transistor in the microwave regime, *Nat. Commun.* **13**, 6104 (2022).